

Residual Semantic Decomposition of Word Embeddings

Seungmin Jin

HSE University

Faculty of Computer Science

Moscow, Russia

sedzhin@hse.ru

Abstract

We introduce Residual Semantic Decomposition (RSD), a neural additive decomposition of word embeddings that balances embedding reconstruction with relational structure preservation. RSD supports recursive binary decomposition: each $K = 2$ fit extracts a local semantic axis, while residuals expose information not absorbed by that axis. In manually specified paired-context diagnostics over ambiguous words, RSD separates supplied context anchors above shuffled-label controls, but entropy diagnostics show that ambiguous targets are not uniformly high-entropy boundary points in static GloVe. We therefore treat residual neighborhoods as qualitative diagnostics rather than benchmark sense predictions.

1 Introduction

Static word embeddings such as GloVe compress rich lexical information into low-dimensional vectors (Pennington et al., 2014). Their geometry reflects corpus co-occurrence structure, including symmetry-driven calendar and time manifolds (Karkada et al., 2026). However, this compression can obscure suppressed or polysemous meanings that remain partially encoded in the relational structure of the vocabulary. Identifying which semantic axes are extracted by a decomposition, and which relations are left unexplained, remains an open diagnostic problem.

Residual-based methods such as PCA and latent semantic analysis reconstruct embeddings from a low-rank basis (Jolliffe, 2002; Deerwester et al., 1990); FADDIS provides an additive relational precedent for decomposing affinity structure (Mirkin and Nascimento, 2012). We propose **Residual Semantic Decomposition (RSD)**, which optimizes embedding reconstruction and relational structure preservation in a single local decomposition. We study RSD as a semantic-axis extraction

procedure, and analyze residuals as diagnostic directions for relations not absorbed by the extracted axes.

Our key observation is that reconstruction residuals can be semantically structured rather than arbitrary noise. For polysemous words like “may” (modal vs. temporal), RSD’s residual direction can retrieve words associated with the contrast context. Unlike multi-prototype or contextual embedding methods that model multiple senses directly (Reisinger and Mooney, 2010; Neelakantan et al., 2014; Peters et al., 2018), we use additive decomposition and residual directions as a post-hoc diagnostic of what a relational decomposition extracts and what it leaves unexplained.

We evaluate this behavior with paired-context diagnostics: each ambiguous word is paired with two manually specified sense contexts, and we ask whether RSD forms a local boundary between the context anchors. RSD separates these anchors above shuffled-label controls, but target entropy shows that ambiguous words are not uniformly high-entropy boundary points in static GloVe. We therefore use residual neighborhoods as qualitative diagnostics rather than benchmark scores.

Our contributions:

- RSD model that extends additive fuzzy relational decomposition with neural assignments and embedding reconstruction.
- Recursive binary semantic-axis extraction procedure based on local $K = 2$ RSD fits and component contrasts.
- Paired-context boundary audit and residual case studies showing when local RSD axes separate manually specified contrast contexts and what residual neighborhoods remain after that separation.

2 Model

RSD decomposes a vocabulary of word embeddings into K relational components. Let $\mathbf{X} \in \mathbb{R}^{N \times D}$ be the embedding matrix for N words, and let $\mathbf{A} \in \mathbb{R}^{N \times N}$ be the cosine affinity matrix where $A_{ij} = \cos(\mathbf{x}_i, \mathbf{x}_j)$. We present RSD as a neural additive decomposition model: like FADDIS, it explains relational structure through fuzzy components, but it also reconstructs the original embedding vectors so that residual directions can be analyzed.

2.1 RSD

RSD uses a soft assignment mechanism via an encoder MLP that maps each embedding to a K -dimensional assignment vector $\mathbf{s}_i \in \mathbb{R}^K$:

$$\begin{aligned} \mathbf{h}_i &= f_\theta(\mathbf{x}_i), \\ s_{ik} &= \frac{\text{softplus}(h_{ik})}{\sum_{\ell=1}^K \text{softplus}(h_{i\ell})}. \end{aligned} \quad (1)$$

The reconstruction and relational objectives are:

$$\begin{aligned} \mathcal{L}_{\text{emb}} &= \|\mathbf{S}\mathbf{C} - \mathbf{X}\|_F^2, \\ \mathcal{L}_{\text{rel}} &= \|\mathbf{S}\mathbf{D}_{\text{rel}}\mathbf{S}^\top - \mathbf{A}\|_F^2, \\ \mathcal{L}_{\text{RSD}} &= \mathcal{L}_{\text{emb}} + \lambda\mathcal{L}_{\text{rel}}. \end{aligned} \quad (2)$$

where $\mathbf{C} \in \mathbb{R}^{K \times D}$ is the basis matrix and $\mathbf{D}_{\text{rel}} \in \mathbb{R}^{K \times K}$ is the relational matrix. For a local binary decomposition ($K = 2$), the component contrast

$$\mathbf{d} = \mathbf{c}_1 - \mathbf{c}_0 \quad (3)$$

is the semantic axis extracted at that node. For any local fit set G , the node-root residual for token i is

$$\mathbf{e}_i^{(G)} = \mathbf{x}_i - \hat{\mathbf{x}}_i^{(G)} = \mathbf{x}_i - \mathbf{s}_i^{(G)}\mathbf{C}^{(G)}. \quad (4)$$

We analyze this error direction as a residual diagnostic. A union-fit residual uses $G = A \cup B$ and asks what remains after the supplied contrast is reconstructed; a source-fit residual uses $G = A$ and scores the target residual against held-out contrast words from B . If a local decomposition explains the dominant axis of an ambiguous token, then a structured residual may point toward semantic relations left unexplained by that axis.

2.2 FADDIS

Mirkin and Nascimento (2012) define an additive fuzzy clustering method for affinity data. Let $\mathbf{U} \in \mathbb{R}^{N \times K}$ be a fuzzy membership matrix and

let $\alpha \in \mathbb{R}_+^K$ be non-negative component weights. The affinity matrix is approximated by a diagonal additive model:

$$\min_{\mathbf{U}, \alpha} \|\mathbf{A} - \mathbf{U} \text{diag}(\alpha) \mathbf{U}^\top\|_F^2. \quad (5)$$

Equivalently, $\hat{A}_{ij} = \sum_k \alpha_k U_{ik} U_{jk}$. RSD keeps this additive relational view but replaces direct membership optimization with encoder-generated assignments, adds explicit embedding reconstruction, and allows a full relational matrix \mathbf{D}_{rel} in Eq. 2.

Residual-comparison note. This relation-only formulation does not define an embedding reconstruction residual: its native output is an affinity reconstruction, not $\hat{\mathbf{X}}$. A post-hoc least-squares decoder from \mathbf{U} to \mathbf{X} would add a new reconstruction step. We therefore restrict direct residual baselines to methods with native embedding reconstructions.

2.3 Residual Probe Setup

All residual probes use the same binary bottleneck ($K = 2$) for RSD, PCA, ICA, and SVD. PCA and ICA are fit on the source-context embedding matrix and reconstructed through their inverse transforms; SVD uses the rank-2 truncated reconstruction. RSD is trained on both the source-context embedding matrix and its cosine affinity matrix. For each method we compute the target residual $\mathbf{e}_i^{(G)}$ and score it by cosine similarity to source-context and contrast-context words. As a negative control, we also score a shuffled non-target residual from the same source-context fit on the same paired-context task.

Note on stability. Seed audits over the six paired-context probes show stable anchor separation but occasional low-informativeness fits, especially for *bank*. The dominant source of variance is the narrow bottleneck (100→2→2), which can collapse for some random seeds. We fix seed=42 for reproducibility and report seed-stability details in Appendix A.

3 Additive Semantic Axis Extraction

RSD uses local binary fits as a semantic-axis extraction trace. At each node, $K = 2$ RSD forms a component reconstruction $\hat{\mathbf{x}}_i^{(G_v)} = s_{i0}\mathbf{c}_0 + s_{i1}\mathbf{c}_1$ and a local contrast $\mathbf{d} = \mathbf{c}_1 - \mathbf{c}_0$. Node-root residual directions $\mathbf{e}_i^{(G_v)} = \mathbf{x}_i - \hat{\mathbf{x}}_i^{(G_v)}$ are retained as lateral diagnostics for information not explained by that split.

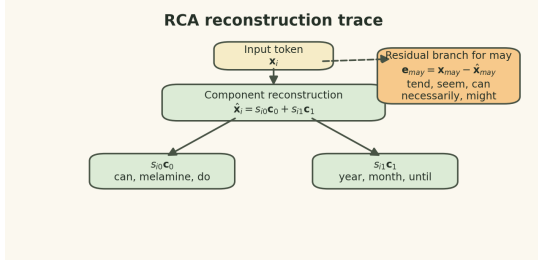


Figure 1: RSD formula trace for the month-name root. The vertical branch shows the component reconstruction \hat{x}_i from two additive components, while the lateral residual branch $e_i^{(G)}$ illustrates the unexplained direction for “may”.

Recursive trace. Given a seed object set G_v , we fit RSD with $K = 2$, compute the local axis $\mathbf{d}_v = \mathbf{c}_1 - \mathbf{c}_0$, label each side by nearest full-vocabulary words to \mathbf{c}_0 and \mathbf{c}_1 , and compute normalized assignment entropy $H(\mathbf{s})/\log 2$. We deepen the trace through component splits only when the split is confident and the node remains underexplained. Node-root residual directions $e_i^{(G_v)}$ are inspected as lateral probes rather than new tree nodes.

We audit this procedure on a controlled vocabulary of 12 month embeddings, using GloVe (Pennington et al., 2014) (100-dim, Wikipedia 2014 + Gigaword 5). Figure 1 shows the reconstruction formula and the lateral residual branch for *may*. The month example is representative of the algorithmic trace; quantitative evidence against cherry-picking is provided by the paired-context evaluation in Section 4.

3.1 Component Axis and Residual Annotation

The root axis separates a broad modal/functional direction from a temporal/contextual direction; its nearest component words are *can, melamine, do, could, you* versus *year, month, until, since, after*. We use normalized assignment entropy $H(\mathbf{s})/\log K$ as a split-confidence diagnostic; the root entropy is 0.070, so the assignment is sharp. The result is not presented as a clean taxonomy because corpus-specific neighbors such as *melamine* appear.

3.2 Residual Direction of “may”

The root residual of “may” retrieves *tend, necessarily, seem, sometimes, often*. This does not imply that *can* is assigned to two disjoint senses; it shows that a residual probe can preserve a sharper token-specific modal direction after the broader compo-

nent axis has explained the dominant relational structure.

Table 1 reports the same root-residual sampling rule for each paired-context target: fit RSD once on the union of the two contexts, compute the target residual, and retrieve its nearest full-vocabulary neighbors.

4 Boundary and Residual Diagnostics

We use the six manually specified paired contexts in Table 1. These probes ask whether a local $K = 2$ RSD fit separates supplied context anchors; they are not a word-sense benchmark. RSD reaches mean anchor AUC 1.000 on the main GloVe-100 probes, versus 0.498 for shuffled labels. A random ambiguous audit from a declared candidate pool (seed=42, 12 targets) gives mean anchor AUC 0.807 versus 0.500 shuffled, with weak cases including *draft, bark, cell, and mouse*. Entropy is cautionary: only *may* has positive target entropy gap in the main audit, and the random sample mean is -0.219 . Across seeds 0–9, *bank* collapses under the informativeness threshold in 40% of runs and *seal* reaches minimum AUC 0.714. Thus boundary scores indicate supplied-contrast separability, not automatic sense discovery.

We report these baselines only to test whether residual scoring depends on RSD rather than any low-rank reconstruction. Root residual neighborhoods remain qualitative: *may* retrieves *tend/necessarily/seem*, while weak cases such as *bank* and *spring* stay near banking or shape/place-name neighborhoods. RSD residuals are therefore diagnostic traces, not direct sense predictions.

5 Related Work

Linear and co-occurrence geometry. Classical dimensionality reduction methods, including latent semantic analysis and PCA/SVD (Deerwester et al., 1990; Jolliffe, 2002), reconstruct embeddings from low-dimensional linear structure. Recent theory shows that symmetries in pairwise co-occurrence statistics can explain calendar, temporal, and geographic manifolds in word embeddings and language-model representations (Karkada et al., 2026). These works describe global geometry; RSD instead locally preserves pairwise relational structure and inspects residual directions as diagnostics.

ICA for embeddings. Independent component analysis (Hyvärinen and Oja, 2000) optimizes sta-

Target	Context A anchors	Context B anchors	Target root residual top words
may	can, could, might, would, should	january, february, march, april, june	tend, necessarily, seem, sometimes, often
march	january, february, april, may, june	walk, parade, stride, step, procession	rally, street, square, demonstration, streets
fall	spring, summer, autumn, winter	drop, descend, decrease, decline, plummet	down, fallen, fell, wall, slipping
spring	summer, autumn, fall, winter	coil, bounce, elastic, mechanism	cone, mound, formation, springs, forming
bank	money, credit, account, deposit, loan	river, shore, stream, coast, lake	hsbc, dresdner, ubs, citibank, suisse
seal	stamp, close, secure, enclose, mark	seals, otter, whale, dolphin, penguin	sealing, sealed, stamped, remove, nail

Table 1: Paired-context diagnostics with up to five non-target context anchors and target residual neighborhoods from the root RSD fit on the union of both contexts. Full anchor lists and per-task diagnostics are reported in Appendix A.

Model	Margin	Pairwise AUC
RSD	0.639	0.948
SVD	0.490	0.880
PCA	0.291	0.778
ICA	0.291	0.778

Table 2: Baseline comparison for source-fit residual scoring. Margin is the mean centroid margin; Pairwise AUC is the probability that held-out contrast anchors outrank source anchors by residual similarity. Higher values are better, but this is a diagnostic comparison, not a benchmark.

tistical independence rather than relational structure preservation. We include ICA to test whether independent latent factors produce residual directions comparable to relational decomposition.

Fuzzy relational decomposition. FADDIS decomposes an affinity matrix as an additive combination of fuzzy components (Mirkin and Nascimento, 2012). RSD keeps this relational perspective but adds embedding reconstruction, which makes residual directions directly available for semantic probing.

Polysemy and contextual meaning. Word-sense induction and multi-prototype embeddings represent ambiguous words with multiple induced senses (Schütze, 1998; Reisinger and Mooney, 2010; Neelakantan et al., 2014; Navigli, 2009). Contextual embedding models represent token meaning in context (Peters et al., 2018). We instead study a narrower diagnostic question: whether residual directions retrieve contrast-associated neighborhoods after relational decomposition of static embeddings.

6 Conclusion

We introduced Residual Semantic Decomposition (RSD), a local decomposition model that balances embedding reconstruction with relational structure preservation. Across paired-context and random ambiguous diagnostics, RSD separates supplied or declared-pool anchors above shuffled controls,

while residual neighborhoods provide qualitative traces of information not captured by the dominant component axis. Future work should improve seed stability, replace declared pools with external benchmarks or corpus-derived contrasts, and validate residual traces against downstream semantic tasks.

Limitations

The experiments are controlled diagnostics, not a full benchmark of word-sense induction. The paired-context tasks are manually constructed and small; anchor AUC values show that supplied context sets are separable by a local RSD axis, not that RSD discovers senses without user-specified contrasts. The random ambiguous audit broadens the probe set, but it is drawn from a declared candidate pool and is not an external benchmark. RSD is also sensitive to random seed initialization due to the narrow encoder bottleneck (2-layer MLP, $100 \rightarrow 2 \rightarrow 2$).

The recursive trace is not a complete semantic graph over the embedding space: component splits deepen local axis decomposition, while residual directions widen local annotations, but the procedure does not close over all pairwise relations or guarantee global consistency. Residual neighborhoods should therefore be read as qualitative diagnostic support, not exact lexical retrieval benchmarks.

References

- Scott Deerwester, Susan T. Dumais, George W. Furnas, Thomas K. Landauer, and Richard Harshman. 1990. [Indexing by latent semantic analysis](#). *Journal of the American Society for Information Science*, 41(6):391–407.
- Aapo Hyvärinen and Erkki Oja. 2000. [Independent component analysis: Algorithms and applications](#). *Neural Networks*, 13(4–5):411–430.
- Ian T. Jolliffe. 2002. *Principal Component Analysis*, second edition. Springer.

- Dhruva Karkada, Daniel J. Korchinski, Andres Nava, Matthieu Wyart, and Yasaman Bahri. 2026. [Symmetry in language statistics shapes the geometry of model representations](#). *Preprint*, arXiv:2602.15029.
- Boris Mirkin and Susana Nascimento. 2012. [Additive spectral method for fuzzy cluster analysis of similarity data including community structure and affinity matrices](#). *Information Sciences*, 183:16–34.
- Roberto Navigli. 2009. [Word sense disambiguation](#). *ACM Computing Surveys*, 41(2):10:1–10:69.
- Arvind Neelakantan, Jeevan Shankar, Alexandre Passos, and Andrew McCallum. 2014. [Efficient non-parametric estimation of multiple embeddings per word in vector space](#). In *Proceedings of the 2014 Conference on Empirical Methods in Natural Language Processing*, pages 1059–1069.
- Jeffrey Pennington, Richard Socher, and Christopher D. Manning. 2014. [GloVe: Global vectors for word representation](#). In *Proceedings of the 2014 Conference on Empirical Methods in Natural Language Processing*, pages 1532–1543.
- Matthew E. Peters, Mark Neumann, Mohit Iyyer, Matt Gardner, Christopher Clark, Kenton Lee, and Luke Zettlemoyer. 2018. [Deep contextualized word representations](#). In *Proceedings of the 2018 Conference of the North American Chapter of the Association for Computational Linguistics: Human Language Technologies*, pages 2227–2237.
- Joseph Reisinger and Raymond J. Mooney. 2010. [Multi-prototype vector-space models of word meaning](#). In *Proceedings of Human Language Technologies: The 2010 Annual Conference of the North American Chapter of the Association for Computational Linguistics*, pages 109–117.
- Hinrich Schütze. 1998. [Automatic word sense discrimination](#). *Computational Linguistics*, 24(1):97–123.

A Supplementary RSD Diagnostics

A.1 Full Paired-Context Anchors

Table 3 lists the complete manually specified anchor sets used in the local boundary audit. The target word is included in both context lists for fitting but excluded from anchor AUC scoring.

A.2 Boundary Diagnostics

Table 4 reports the GloVe-100 local boundary audit. Anchor AUC is computed over non-target anchors after orienting $b_i = s_{i1} - s_{i0}$ so Context B has larger mean score.

A.3 Random Ambiguous Audit

The random ambiguous audit is drawn from a declared candidate pool rather than WordNet or another external resource. The pool is: bat, bark, bass, cell, charge, club, crane, draft, jam, match, mouse, organ, palm, pitch, plane, port, ring, scale, sentence, yard. The seed=42 sample is cell, bat, jam, draft, ring, bass, organ, bark, mouse, scale, palm, crane.

A.4 Seed Stability Audit

Table 6 repeats the six main boundary audits over seeds 0–9. Anchor separation is stable, but assignment informativeness can collapse for some seeds; we mark a collapse when informativeness is below 0.02.

A.5 Root Residual Neighborhoods

Table 7 shows RSD root residual neighborhoods. For each target, RSD is fit once on the union of the two context-anchor sets, and the table reports nearest full-vocabulary words to $\mathbf{e}_t^{(A \cup B)}$. These are qualitative diagnostics, not exact lexical retrieval scores.

A.6 May Three-Step Trace

Table 8 gives a compact may three-step trace from the residual-branch sampler. This is included to make the diagnostic procedure auditable; it is not a complete semantic graph.

A.7 Embedding Robustness

The multi-embedding audit repeats the same six paired-context tasks over GloVe 50/100/200/300 and fastText 300d. Mean anchor AUCs are 1.000, 1.000, 1.000, 0.939, and 0.887 respectively, while shuffled-label means remain near chance (0.498–0.500). GloVe-300 and fastText have much lower

assignment informativeness, so robustness should be read as above-shuffle anchor separation rather than uniformly sharp decomposition.

Target	Context anchors
may	A: can, could, might, would, should, may, must, possibly, perhaps, maybe B: january, february, march, april, may, june, july, august, september, october, november, december
march	A: january, february, march, april, may, june, july, august, september, october, november, december B: walk, parade, stride, step, procession, march
fall	A: spring, summer, autumn, fall, winter B: drop, descend, decrease, decline, plummet, fall
spring	A: spring, summer, autumn, fall, winter B: coil, bounce, elastic, mechanism, spring
bank	A: bank, money, credit, account, deposit, loan, financial, investment, savings B: river, shore, stream, coast, lake, bank, water, shoreline, embankment
seal	A: stamp, close, secure, seal, enclose, mark B: seal, seals, otter, whale, dolphin, penguin, marine, turtle

Table 3: Full paired-context anchors.

Task	AUC	Shuffle	ΔH_t	Emb. err.
may	1.000	0.494	0.050	0.332
march	1.000	0.494	-0.223	0.396
fall	1.000	0.501	-0.360	0.607
spring	1.000	0.497	-0.401	0.585
bank	1.000	0.502	-0.236	0.671
seal	1.000	0.499	-0.291	0.780

Table 4: Boundary diagnostics for the main GloVe-100 audit. ΔH_t is target entropy minus mean anchor entropy.

Task	AUC	Shuffle	ΔH_t	Info.
cell	0.562	0.489	-0.429	0.041
bat	0.812	0.510	-0.404	0.064
jam	1.000	0.497	-0.080	0.032
draft	0.438	0.500	-0.013	0.033
ring	1.000	0.496	-0.155	0.014
bass	1.000	0.503	-0.383	0.039
organ	1.000	0.501	-0.288	0.050
bark	0.438	0.507	-0.188	0.031
mouse	0.625	0.496	-0.480	0.017
scale	0.875	0.505	0.040	0.024
palm	0.938	0.497	-0.089	0.039
crane	1.000	0.495	-0.160	0.015
Mean	0.807	0.500	-0.219	0.033

Table 5: Random ambiguous audit over a fixed seed=42 sample from the declared candidate pool.

Task	Mean AUC	Min AUC	Collapse rate
may	1.000	1.000	0.000
march	1.000	1.000	0.000
fall	0.970	0.900	0.000
spring	1.000	1.000	0.000
bank	0.989	0.938	0.400
seal	0.966	0.714	0.000

Table 6: Seed stability audit for RSD boundary metrics over seeds 0–9.

Task	Top root residual words
may	tend, necessarily, seem, sometimes, often
march	rally, street, square, demonstration, streets
fall	down, fallen, fell, wall, slipping
spring	cone, mound, formation, springs, forming
bank	hsbc, dresdner, ubs, citibank, suisse
seal	sealing, sealed, stamped, remove, nail

Table 7: RSD root residual neighborhoods, including weak cases.

Step	Node	Component 0 words	Component 1 words
1	months root; may residual words: tend, seem, can, necessarily, might	can, melamine, do, could, you	year, month, until, since, after
2	seem, tend, can, necessarily, might	do, you, they, we, could	melamine, ink, ote, taxonomy, tinto
3	part, same, this, next, new	be, an, its, the, that	tinto, bhp, billiton, uranium, contract

Table 8: Compact RSD residual-branch trace used for the may diagnostic.